Afyon Kocatepe Üniversitesi
FEN BİLİMLERİ DERGİSİ

2(1) 121-134
2000

Afyon Kocatepe University
JOURNAL OF SCIENCE

DECENTRALISED PID LOAD FREQUENCY CONTROLLER DESIGN BASED ON INTERACTION MARGIN

Hasan ÇİMEN

AKÜ, Technical Education Faculty, AFYON

ABSTRACT

The decentralised load-frequency controller design problem concerned is translated into controller design for a multi-input multi-output (MIMO) control system.

It is shown that, subject to condition based on the structured singular values, each local controller can be designed independently. The stability condition for the overall system can be stated as to achieve a sufficient interaction margin and a sufficient gain and phase margin defined in classical feedback theory during each independent design.

It is demonstrated by computer simulations that within this general framework, PID local controllers can be designed to achieve satisfactory performances for a sample two-area power system.

Key Words: PID, load-frequency control, robustness, decentralised control

LOKAL PID YÜK-FREKANS KONTROLÖR DİZAYNI

ÖZET

Yerel yük-frekans kontrolör dizayn problemi çok girişli ve çok çıkışlı çok bölgeli sistemler için eşdeğer yerel kontrolör dizayn problemine dönüştürüldü.

Yapılandırılmış tekil değerlerle ilgili bir şarta bağlı olarak bağımsız yerel kontrolörlerin dizay edilebileceği gösterildi. Bu şart tüm sistemin stabilite şartı için belirli bir karşılıklı etkileşim sınırı olarak belirlendi. Bu genel yaklaşım içinde

bilgisayar simülasyonları gösterdi ki her bir bölge için bağımsız PID kontrolörleri dizayn edilebilir ve yeterli bir performans sağlanır.

Anahtar Kelimeler: PID, yük-frekans, sağlam, yerinden kontrol

1. INTRODUCTION

In the load-frequency control function, it is necessary that the system frequency and the inter-area tie-line power be kept as near to the scheduled values as possible through control action. The important requirement for system stability may be conveniently met by adopting a global policy for design, based for example on well-established principles of pole placement or optimal control by state feedback. Where such an approach is to be used with decentralised control, the state vector for the entire system should be made available for the generation of local feedback control signals in all areas. This requirement may be met if a reconstruction of the whole system state vector is observable from the area measurements. However, even if the observability condition satisfied, the resulted controllers with appropriately designed observers are normally quite complicated and this approach is not suitable for a large power system where the total number of the state variables large [1].

It is known that, although the LFC for multi-area power systems can be naturally formulated as a large-scale system decentralised control problem, it can be translated into an equivalent problem of decentralised controller design for a multi-input multi-output (MIMO) control system [5].

Decentralised PID control is one of the most common control schemes for interacting multi-input multi-output (MIMO) plants in process industries. The main reason for this is its relatively simple structure, which is easy to understand and to implement. In a case of actuator or sensor failure, it is relatively easy to stabilise manually because only one loop is directly effected by the failure. As given in reference [11], there are still many difficulties on designing PID controllers in MIMO systems. Only limited number of works addressed the designing decentralised PID controllers. Despite the wide popularity of decentralised PID control, the number of applicable manual tuning methods is limited. Even for single-input single-output (SISO) systems the tuning of a PID controller is not easy task. The fundamental step in that method is the

identification of critical gain and critical frequency of the plant, which togetherare commonly called the critical point. Based on these values, the controller gain and the integral and derivative coefficients are calculated. In MIMO systems the choosing PID parameters problem is more complicated due to the interactions between loops. A change of a single parameter affects, in general, all other loops as well.

Recently, structured singular values μ are used in a different way from those commonly used in the robust control literature [12]. It is shown that subject to a condition based on μ, each local area controller can be designed independently. The stability condition for power systems with local area controllers can be stated as to achieve a sufficient interaction margin proposed in [5] and sufficient gain and phase margin defined in classical feedback theory during each independent design. It is shown that within this framework it is possible to design very simple local area controllers, such as PID, to achieve satisfactory system performances.

2. SAMPLE MULTI-AREA POWER SYSTEM

Figure 1 shows a block diagram for the load-frequency control of a two-area power system, which have been used by most researchers. State-space representation of this model has been widely used for the investigation of different methods [1, 2, 4, 6, 8, 9]. The nomenclature used and the nominal parameter values, in per unit (pu), are given in Appendix.

A state-space model for the system of Figure 1 can be constructed as

$$\dot{\mathbf{x}} = \mathbf{A}\mathbf{x} + \mathbf{B}\mathbf{u}$$

$$\mathbf{y} = \mathbf{C}\mathbf{x}$$

where $\mathbf{u} = [u_1 \quad u_2]^T$; $\mathbf{y} = [y_1 \quad y_2]^T = [\Delta f_1 \quad \Delta f_2]^T$;

$$\mathbf{x} = [\Delta f_1 \quad \Delta P_{T1} \quad \Delta P_{G1} \quad \Delta P_{c1} \quad \Delta P_{tie} \quad \Delta f_2 \quad \Delta P_{T2} \quad \Delta P_{G2} \quad \Delta P_{c2}]^T$$

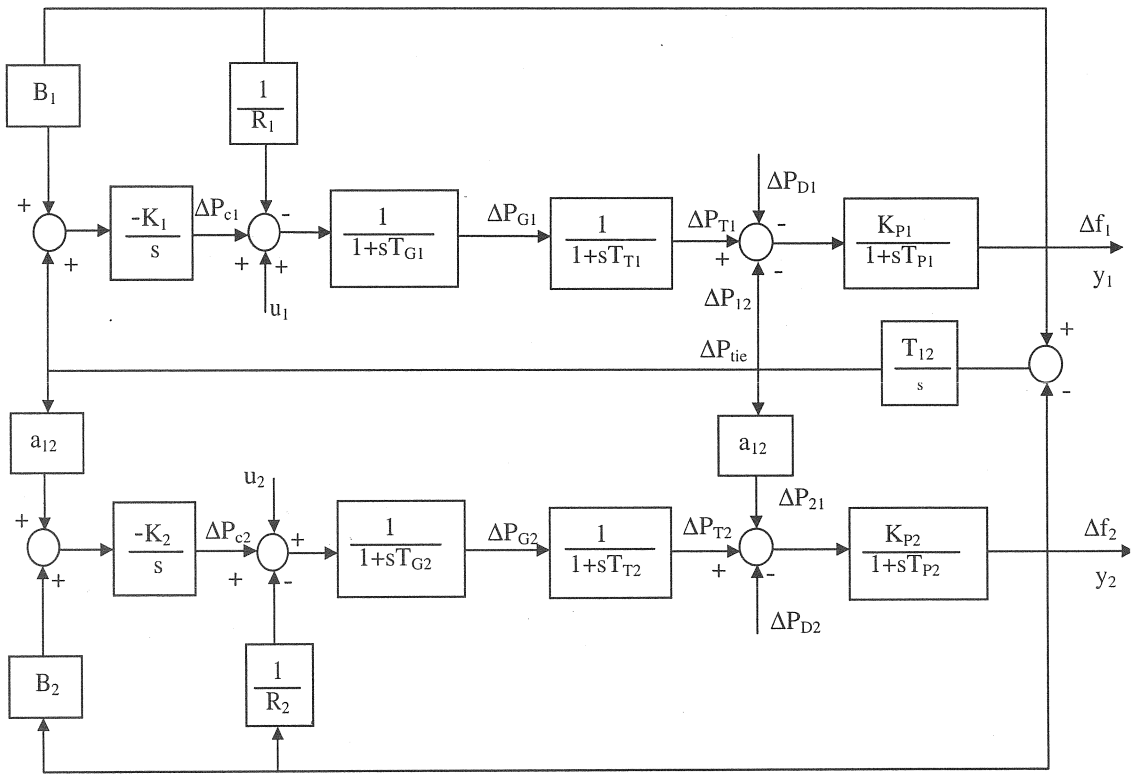

Fig. 1. Block diagram of two-area system

The system is stable and the control task is to minimise the system frequency deviation Δf_1 in area 1, Δf_2 in area 2 and the deviation in the tie-line power flow ΔP_{tie} between the two areas under the load disturbances ΔP_{D1} and ΔP_{D2} in the two areas. Since the system parameters for the two areas are identical and the ΔP_{tie} is caused by $\Delta f_1 - \Delta f_2$, the system performance can be mainly tested by applying a disturbance ΔP_{D1} to the system and observing the time response of Δf_1. Some simulation results for Δf_1 when a step disturbance of $\Delta P_{D1} = 0.01\,\text{pu}$ is applied to the system are plotted in Figures. 5, 6 and 7 as dashed lines.

3. INTERACTION MARGIN

A transfer function $\mathbf{G}(s) = \left[g_{ij}(s)\right]_{i,j=1,2,...m}$ for a $m \times m$ MIMO plant is decomposed into

$$\mathbf{G}(s) = \tilde{\mathbf{G}}(s) + \hat{\mathbf{G}}(s) \quad (1)$$

where $\tilde{\mathbf{G}}(s) = diag[g_{ii}(s)]_{i=1,2...m}$ is diagonal matrix; all diagonal elements in $\hat{\mathbf{G}}(s)$ are zeros and off-diagonal elements in $\hat{\mathbf{G}}(s)$ are equal to those in $\mathbf{G}(s)$. Using the notations

$$\mathbf{E}(s) = \hat{\mathbf{G}}(s)\tilde{\mathbf{G}}^{-1}(s) \quad (2)$$

$$\tilde{\mathbf{H}}(s) = \tilde{\mathbf{G}}(s)\mathbf{F}(s)(\mathbf{I} + \tilde{\mathbf{G}}(s)\mathbf{F}(s))^{-1} = diag[h_i(s)] \quad (3)$$

$$\mathbf{H}(s) = \mathbf{G}(s)\mathbf{F}(s)(\mathbf{I} + \mathbf{G}(s)\mathbf{F}(s))^{-1} \quad (4)$$

where $\mathbf{F}(s) = diag[f_i(s)]_{i=1,2,...m}$ is a diagonal transfer function for a decentralised controller; $\tilde{\mathbf{H}}(s)$ or $\mathbf{H}(s)$ is a closed-loop transfer function matrix for a feedback system consisting of $\mathbf{F}(s)$ and , $\tilde{\mathbf{G}}(s)$, or $\mathbf{F}(s)$ and $\mathbf{G}(s)$, respectively. The following theorem were proved in [10]:
The closed-loop system $\mathbf{H}(s)$ is stable if

(c-1) $\mathbf{G}(s)$ and $\tilde{\mathbf{G}}(s)$ have the same number of right half-plane poles

(c-2) $\tilde{\mathbf{H}}(s)$ is stable, and

(c-3) $\left|h_i(jw)\right| < \mu^{-1}(\mathbf{E}(jw)) \forall w (i = 1,2,...m)$

where $|\ |$ denotes the magnitude and μ denotes Doyle's structured singular value with respect to the decentralised controller structure of $\mathbf{F}(s)$.

This theorem gives sufficient conditions for the system $\mathbf{H}(s)$ to be stable if the controller design based on the fully non-interactive model $\tilde{\mathbf{G}}(s)$, i.e. each $f_i(s)$ is designed, independently, based on an SISO model $g_{ii}(s)$. In particular, condition (c-3) states that the magnitude of the frequency response of

SISO closed-loop transfer function $h_i(s) = f_i(s)g_{ii}(s)/(1 + f_i(s)g_{ii}(s))$ must be less than the value of a scalar frequency dependent function $\mu^{-1}(\mathbf{E}(jw))$. Grosdidier and Morar have also proved that [10] although (c-3) is a sufficient condition and therefore may have some conservativeness, compared with other conditions developed for the independent decoupled design, for example the diagonal dominant condition, (c-3) gives the tightest restrictive band and is the least conservative.
Before applying these results to our system, it is necessary to consider the issue of the robust stability. The stability condition (c-4) is given for the nominal plant $\mathbf{G}(s)$. If the state space model of (1) changes, the plant model $\mathbf{G}(s)$ will also change. It is generally not possible to establish a clear relationship between the change of values involved in (1) and the change of values involved in condition (c-3). The stability condition were specified in [5] as:

(r-1) Condition (c-4) is satisfied with a sufficient margin. This can be checked by plotting $|h_i(jw)|$ and $\mu^{-1}(\mathbf{E}(jw))$ on the same graph and an interaction margin for loop *i* can be defined as the shortest vertical distance between the two curves.

(r-2) There are sufficient gain and phase margins in each SISO loop for the stability. This can be also checked by Bode or Nyquist plot of $f_i(jw)g_{ii}(jw)$.

4. LOCAL AREA CONTROLLER DESIGN

Within the general framework of the independent design subject to some conditions given in Section 3, PID controller design method can be applied to the local area load-frequency controller design.

The frequency response of a system indicates the magnitude and phase relationship between the sinusoidal inputs to a linear system generates sinusoidal responses of the same frequency as the input signal, but possibly with different amplitude and phase. In the design of linear control systems using frequency-domain methods, the performance of a system can be identified using the appropriate performance measures such as phase margin, gain margin, resonant

peak and bandwidth. These frequency domain specifications also give some relative information about the time-domain specifications, such as a large bandwidth corresponds to a faster rise time.

A PID controller would add damping to a system, but the steady-state response is not affected; the PI controller could add damping and improve the steady-state error at the same time, but the rise time and settling time are penalised. This leads to the motivation of using a PID controller so that the best properties of each of the PI and the PD controllers are utilised. The following approach is outlined in [14] as a possible means of designing the PID control for a control system.

Consider that the PID controller consists of a PI portion connected in cascade with a PD portion. The PID-controller transfer function is written as

$$G_c(s) = K_p + K_D s + K_I / s = (K_{P1} + K_{D1} s)(K_{P2} + K_{I2} / s) \quad (5)$$

Equating both sides of Equation (5), we have

$$\begin{aligned} K_P &= K_{P1}K_{P2} + K_{P1}K_{I2} \\ K_D &= K_{D1}K_{P2} \\ K_I &= K_{I2}K_{P1} \end{aligned} \quad (6)$$

After we get PD parameters proportion and derivative (K_{P1} and K_{D1}). PI parameters (K_{P2} and K_{I2}) are calculated. Frequency domain procedure for PI compensation to realise a given phase margin is as follows:

1. The Bode plot of the open-loop transfer function $\mathbf{G_P}(s)$ of the uncompensated system is made with the open-loop gain set according to the steady-state performance requirement.

2.The phase margin and the gain margin of the uncompensated system are determined from the Bode plot. For a certain specified phase margin, the new gain-crossover frequency w_c' corresponding to this phase margin is found on the Bode plot. The magnitude plot of the compensated transfer function must pass through the 0-dB axis at this new gain-crossover frequency in order to realise the desired phase margin.

3.To bring the magnitude curve of the uncompensated transfer function down to 0 dB at the new gain-crossover frequency w_c' the PI controller must provide the amount of attenuation equal to the gain of the magnitude curve at the new gain-crossover frequency. In other words, set

$$\left|G_P(jw_C')\right|_{dB} = -20\log_{10} K_{P2} \qquad K_{P2}<1 \tag{7}$$

from which

$$K_{P2} = 10^{-\left|G_P(jw_c')\right|_{dB}/20} \qquad K_{P2}<1 \tag{8}$$

Once the value of K_{P2} is determined, it is necessary only to select the proper value of K_{I2} to complete the design. It is apparent that if the corner frequency $w=K_I/K_P$ is placed far below the new gain-crossover frequency w_c [14]. We set

$$\frac{K_{I2}}{K_{P2}} = \frac{w_c'}{10} \quad rad/sec \tag{9}$$

thus,

$$K_{I2} = \frac{w_c'}{10} K_{P2} \quad rad/sec \tag{10}$$

4.The values of K_{P1}, K_{D1}, K_{I2} and K_{P2} are substituted in (5) to give the desired transfer function of PID controller.

According to the design approach above, PD parameters of K_{P1}=0.25 and K_{D1}=0.25 are obtained by trial and error to increase phase and gain margins for two-area system given in Section 2. Applying frequency domain procedure for PI compensation, K_{I2}= 0.2191 and K_{P2}= 0.7049 values are calculated. Using Equations in (6) K_P=0.2310, K_D=0.1762 and K_I=0.0548 parameters are found.

The frequency response of $f_1(s)g_{11}(s)$ is given in Figure 2 as solid lines. The gain margin is increased from 5.8 *dB* to 291.2 *dB* and phase margin is increased from 14.03 *degree* to 91.77 *degree.*

The frequency response of

$$h_1(s) = \frac{f_1(s)g_{11}(s)}{1+f_1(s)g_{11}(s)} \tag{11}$$

is given in Figure 3 as dotted-dashed line. $h_1(s)$ can be obtained by first connecting the PID controller to the state-space model used to calculate $g_{11}(s)$, (the **A** matrix, the first column of the **B** matrix and the first row of the **C** matrix in (1)), then finding the resulted closed-loop system transfer function. The interaction margin obtained is 2.37 dB at a frequency w=2.95 *rad/sec*.

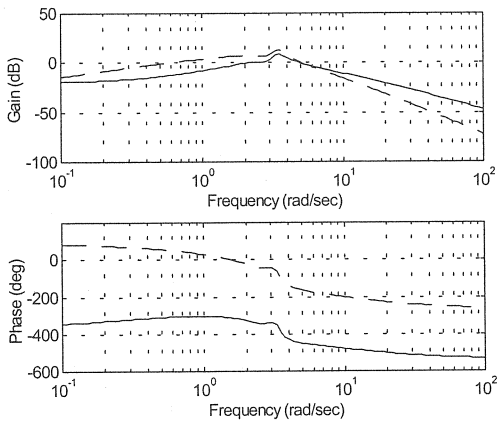

Figure 2. Bode plot of $f_1 g_{11}(s)$ (solid line) and $g_{11}(s)$ (dashed line)

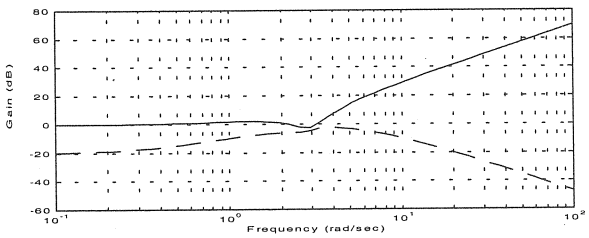

Figure 3. Bode plot of $\mu^{-1}(\mathbf{E}(jw))$ (solid line) and h_1 (dashed line)

Table 1. j_{tie} values

Test No	Parameter Changes %	Case A	Case B
0	0	3.5	11.6
1	+5	3.2	16.3
2	-5	3.6	8.4
3	+10	3.1	23.4
4	-10	3.5	6.5
5	+15	3.0	32.8
6	-15	3.9	4.9
7	+20	2.9	45.7
8	-20	4.1	4.4
9	+25	2.9	64.9
10	-25	4.2	4.9
11	+30	3.0	89.1
12	-30	6.3	5.4

Table 2. j_{tie} values

Test No	Parameter Changes %	Case A	Case B
0	0	2.3	4.2
1	+5	2.3	5.5
2	-5	2.3	3.3
3	+10	2.3	7.7
4	-10	2.2	2.8
5	+15	2.3	11.1
6	-15	2.3	2.5
7	+20	2.3	15.8
8	-20	2.3	2.3
9	+25	2.3	22.4
10	-25	2.2	2.3
11	+30	2.3	30.6
12	-30	2.3	2.4

5. SIMULATION RESULT

To test system performance, a step load disturbance of ΔP_{D1}=0.01 pu is applied to area 1 and the system output of Δf_1 is observed. An integration-absolute-error-time (IAET) criteria of the following form is also use

$$j_{fre} = 1000 \int_0^{20} |\Delta f_1(t)| t dt$$

In the simulation study, the linear model of a nonreheating turbine $\Delta P_T / \Delta P_G$ in Figure 1 is replaced by a non-linear model with δ=0.010. This is to take into account the generating rate constrains, i.e. the practical limit on the response speed of a turbine, which was not considered in some early publications [8,9].

A number of simulations, using the nominal plant parameters and those with all plant parameters changed by some percentage, have been carried out for two different cases. The j_{fre} values obtained are listed in Table 1, where
Case A: no additional controller is connected to two-area system [5], and

Case B: two identical PID controllers designed in Section 4 are added to the system.

Some selected time response plots are given in Figures 4, 5, and 6; dashed lines are for Case A and solid lines are for Case B. Similarly, the deviation in the tie-line power flow ΔP_{tie} between two areas under the load disturbance ΔP_{D1}=0.01pu is also checked. An IAET criteria of the following form is used and the results for the two cases are given in Table 2.

$$j_{tie} = 1000 \int_0^{20} |\Delta P_{tie}(t)| t dt$$

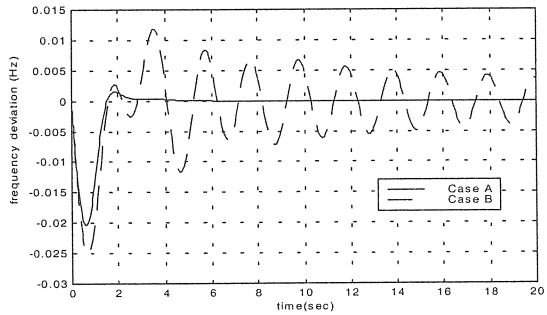

Figure 4. Dynamic response of Δf_1 for Test 0

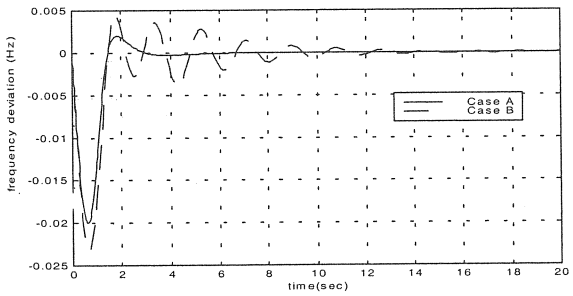

Figure 5. Dynamic response of Δf_1 for Test 11

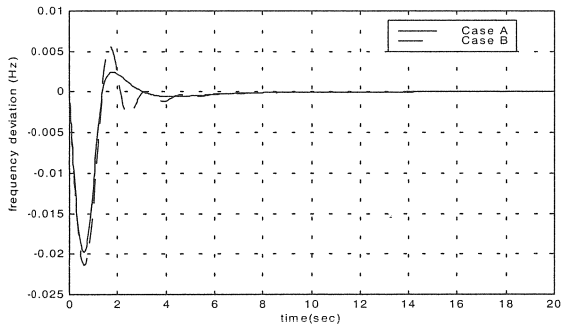

Figure 6. Dynamic response of Δf_1 for Test 12

It can be seen in Tables 1 and 2 and Figures 4, 5, and 6 that simple PID controllers designed based on interaction margin improve system performances. Two PID controllers designed in this study give better responses than conventional controllers. Simulation results of Case A, and Case B in Table 1, values of j_{fre} change between 2.9 and 6.3 for Case A while performance indices for Case B Change between 4.4 and 89.1. Also we can see this improvement in Table 2 j_{tie} values listed in column of Case B, which are between 2.2 and 2.3.

These improvements over Case B show that decentralised PID controllers designed by the method given in this paper not only improve system performance but also this performance is robust against the plant parameter changes.

6. CONCLUSION

A decentralised PID load-frequency controller design approach has been proposed. In this study, it is shown that , under the proposed general frame work, relatively simple local controller design methods such as the PID controller can be applied to the decentralised load frequency control problem. Using interaction margin, each local controller can be designed independently even with simple design methods. It is not necessary to observe whole system. Due to the nature of 'independent design subject to some conditions', the

proposed design approach and the methods can be applied to a general *m*-area power system.
For a given system, it is not easy to specify the required sufficient margins stated in conditions (r-1) and (r-2) to guarantee the stability of the system under plant parameter changes. This presents a theoretical problem to be further investigated by control theoretics. Decentralised PID controller parameters may be tuned subject to interaction and for this, a systematic may be investigated.

7.REFERENCES

1. Aldeen, M. and J.F. Marsh, Decentralized proportional plus integral design method for interconnected power systems, *IEE Proc-C*, **138**, 263-274 (1991).

2. Al-Hamouz, Z.M. and Y.L. Abdel-Majid, Variable structure load frequency controller for multi-area power systems, *Int. J. Electrical Power and Energy Systems*, **15,** 293-300 (1993).

3. Atherton P. D., PID controller tuning. *Computing & Control Engineering Journal*, April,44-50 (1999).

4. Bengiamin, N. N. and W. C., Variable structure control of electric power generation. *IEEE Trans.*, **PAS-101**, 376-380 (1982).

5. Çimen, H. and T.C. Yang, Applying structured singular values to decentralised load –frequency control, *UPEC'96, 31st Universities Conference, Iraklio*, **3,** 993-996 (1996)..

6. Feliachi, A Optimal decentralised load-frequency control, *IEEE Trans.*, **PWRS-2**, 379-386 (1987).

8. Fosha, C. E. and O. I. Elgerd , The megawatt-frequency control problem: a new approach via optimal control theory. IEEE Trans., **PAS-89**, 563-573 (1970).

9. Geromel J.C. and P. L. D. Peres, Decentralised load-frequency control. *IEE Proc. D*, **132**, 225-230 (1985).

10. Grosdidier, G. and M. Morari, Interaction measures for system under decentralized control, *Automatica*, **22**,309-319 (1986).

11. Halevi Y., Z. Y. Palmar and T. Efrati, Automatic tuning of decentralized PID controllers for MIMO processes, *J. Proc. Cont.*, **7**, 119-128 (1997).

12. Hammond, P.H., *Robust Control System Design Using H_∞ and Related Methods*, Institute of Measurement and Control, LONDON (1991).

13. Hiyama, T., Design of decentralised load frequency regulators for interconnected power systems, *IEE Proc. C.*, **129**, 17-23 (1982).

14. Kuo, B. C., *Automatic control systems* 6th edition, Prentice-Hall Englewood Cliffs, (1990).

15. Liaw, C. M., Design of a reduced –order adaptive load frequency controller for a interconnected hydrothermal power system. *Int. J. Control*, **60**, 1051-1068 (1994)..

16. Pan, C.T. and C.M. Liaw, An adaptive controller for power system load frequency control. *IEEE Trans.*, **PWRS-4**, 122-127 (1989).

17. Skogestad, S. and I. Postlethwaite, *Multivariable Feedback Control Analysis and Design*. John Wiley & Sons, Chichester (1996).

18. Wang Q.G., B. Zou, T. H. Lee and Q. Bi Auto-tuning of multivariable PID controllers from decentralized relay feedback. *Automatica*, **33**, 319-330 (1997).

8.APPENDIX

T_T turbine time constant $T_{T1}=T_{T2}=0.3$;T_G governor time constant $T_{G1}=T_{G2}=0.08$; T_p power system time constant $T_{P1}=T_{P2}=20$ sec; R regulation parameter $R_1=R_2=2.4$ Hz/puMW ; K_p power system gain $K_{p1}=K_{p2}=120$Hz/puMW; T_{12} synchronising coefficient $T_{12}=0.545$puMW ; B frequency bias parameter $B_1=B_2=0.425$puMW/Hz; P_D load disturbance, K integration gain $K_1=K_2=1$; a_{12} ratio between the base values of two area, $a_{12}=-1$